

# EFFECT OF SPACE CHARGE ON EXTRACTION EFFICIENCY OF IONS IN CYCLOTRON GAS STOPPER\*

Y.K.Batygin<sup>#</sup>, G.Bollen, C.Campbell, F.Marti, D.J.Morrissey, G.Pang, S.Schwarz, NSCL, Michigan State University, East Lansing, MI 48824, USA

## Abstract

The cyclotron gas stopper is a newly proposed device to stop energetic rare isotope ions from projectile fragmentation reactions in a helium-filled chamber [1, 2]. The radioactive ions are slowed down by collisions with a buffer gas inside a cyclotron-type magnet and are extracted via interactions with a Radio Frequency field applied to a sequence of concentric electrodes (RF carpet). The present study focuses on a detailed understanding of space charge effects in the ion extraction region. The space charge is generated by the ionized helium gas created by the stopping of the ions and eventually limits the beam rate. Particle-in-cell simulations of a two-component (electron-helium) plasma interacting via Coulomb forces were performed in the space charge field created by the stopping beam.

## INTRODUCTION

The cyclotron gas stopper is a device for the deceleration of radioactive ions created by the projectile fragmentation (see Fig. 1). The fast ions ( $\sim 100$  MeV/u) are injected into a helium-filled chamber inside a vertical magnetic field where they immediately enter a solid degrader so that they can be captured by the magnetic field. The fast ions lose the remainder of their kinetic energy in collisions with the helium buffer gas. This process ionizes the helium atoms. A vertical electric field is used to remove electrons and move positively charged ions to the RF-carpet. At high incoming particle rates, the amount of ionization becomes so large that the stopped ions cannot be completely removed. As a result, a neutralized plasma accumulates in the center of the stopping chamber and additional fast ions are not or are only slowly extracted because they come to rest in the plasma-shielded region. This present work analysed the overall process of charge migration to provide estimates of the maximum incoming particle rate.

## NUMERICAL METHOD

Present simulations are based on a preceding detailed numerical study of rare isotope production, transport, and stopping in a gas-filled magnetic field [1]. The program LISE++ [3] was used to calculate the transmission, yields, and ion-optical properties of the projectile fragment beam. A C++ version of the ATIMA code [4] was used to calculate the energy lost by the incoming beam in the solid degrader. The Stopping and Range Tables from the SRIM package [5] were used to calculate the energy loss in the helium gas. The CycStop code [6] combined this input to calculate the fast ion stopping

\*Work supported by the US Department of Energy under Contract No DE-FG02-06ER41413

<sup>#</sup>batygin@nsl.msu.edu

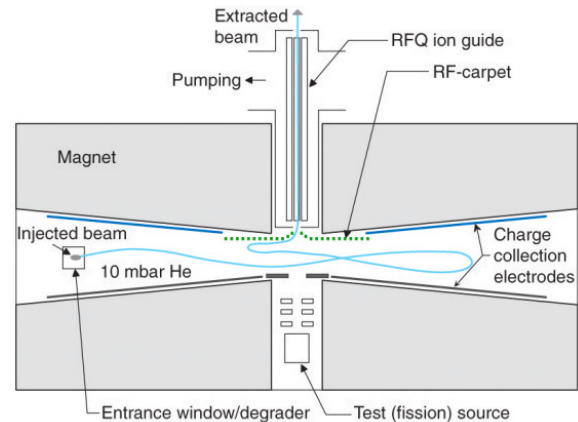


Figure 1: Schematic layout of cyclotron gas stopper [1]. The fast projectile fragments are incident horizontally at the left and after stopping are dragged to the center for axial extraction.

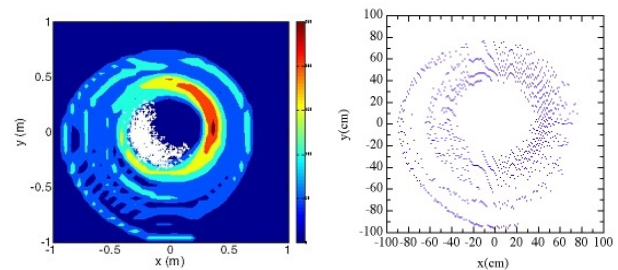


Figure 2: (Left) Top view of the energy loss density in color and the positions of the stopped ions in white, and (right) the distribution of  $e^-/He^+$  ion-pairs created by the stopping of a  $^{79}Br$  beam from the CycStop code [6].

distribution, the losses, and the spatial deposition of energy in the helium. The energy distributions were the input for the space charge phenomena in the present work (see Fig. 2).

The calculation of space charge effects in  $e^-/He^+$  plasma were performed with a modified version of the BEAMPATH code [7]. The simulations were performed by simultaneous tracking of  $He^+$  and electrons in the field created by their own space charge forces,  $\vec{E}_{sc}$ , and applied external electric field,  $\vec{E}_o$ , with a velocity  $\vec{v}$  given by

$$\vec{v} = k(\vec{E}_o + \vec{E}_{sc}), \quad (1)$$

where  $k$  is the mobility of ion or electron. The mobility of  $He^+$  ions at room temperature and pressure of  $P = 200$  mbar was taken as  $k_{He^+} = 10^5$  cm<sup>2</sup>/(kVs) and is inversely proportional to gas pressure. The mobility of electrons is typically three orders of magnitude higher than that of

$He^+$  under the same conditions. However, direct simulation of  $e^-/He^+$  plasma with such large differences in ion mobilities is problematic due to the dramatic difference in the time scales of the dynamics of electrons and  $He^+$ . Therefore, in the present work the mobility of the electrons was artificially reduced by a factor of ten to  $10^7 \text{ cm}^2/(\text{kVs})$  to simultaneously follow the motion of the ions and electrons in the same calculation.

Radioactive ions were injected into the gas at a rate of  $dN/dt_{in}$ . Each incoming radioactive ion created a cloud of  $He^+$  and electron charge at the rate  $dQ/dN$ , each. The product of these two rates gives the rate of creation of  $He^+$  and electrons in the gas-filled chamber  $dQ/dt = (dN/dt_{in})(dQ/dN)$ . The simulation time step,  $\Delta t = \Delta T/N_{step}$ , was defined as a ratio of the simulation period,  $\Delta T$ , and the number of integration steps,  $N_{step}$ . At each integration step the entire spatial distribution of  $e^-/He^+$  particles was injected into the system such that the incoming charge of each component was  $\Delta q = (dQ/dt) \Delta t$ . This distribution is added to that remaining from the previously injected particles (see Fig. 3). The electrons and positive ions move in opposite directions in the net field created by applied collection field and by their space charge.

The space charge field was calculated by the numerical solution of Poisson's equation in two-dimensional cylindrical coordinates:

$$\frac{1}{r} \frac{\partial}{\partial r} \left( r \frac{\partial U}{\partial r} \right) + \frac{\partial^2 U}{\partial z^2} = - \frac{\rho(r, z)}{\epsilon_0}, \quad (2)$$

where  $\rho(r, z)$  is the instantaneous value of charge density of the electrons and ions present in the system. The Dirichlet boundary conditions at the surface of a tube of radius  $a$ , and the Neumann condition at the axis were applied. While a new fraction of  $e^-/He^+$  was injected into the system at each time step, some fraction of particles was removed in the extraction region and by the walls of the gas cell. Poisson's equation was solved by Fourier transformation in the  $z$ -direction and solution of a three-diagonal matrix equation in radial direction.

## SIMULATION RESULTS

Fig. 3 illustrates the dynamics of  $e^-/He^+$  cloud formation for the injection of  $^{79}\text{Br}$  ions into the system with an axial electric field of  $E_0=10 \text{ V/cm}$  for an incoming particle rate of  $dN/dt_{in} = 10^5 \text{ part/sec}$  and energy of  $E = 1.69 \cdot 10^9 \text{ eV}$ . The number of  $e^-/He^+$  pairs per stopped ion is  $N = E/E_i = 4.23 \cdot 10^7$  where  $E_i = 40 \text{ eV}$  is the effective ionization potential in helium gas. Each incoming beam particle creates  $e^-/He^+$  pairs equal to  $dQ/dN = 6.76 \cdot 10^{-12} \text{ C/part}$  so that the increase in charge due to  $e^-/He^+$  pairs in the system is  $dQ/dt = 6.76 \cdot 10^{-7} \text{ C/s}$ . As illustrated in Fig. 3, shortly after starting the injection of beam, the electrons quickly travel to the anode wall of gas cell at  $z = 10 \text{ cm}$  (the right edge in this view). After  $t = 5 \cdot 10^{-3} \text{ sec}$ , the system has relaxed to steady-state condition for this beam rate. Under these conditions the outgoing particle rate is equal to incoming rate  $dN/dt_{out} =$

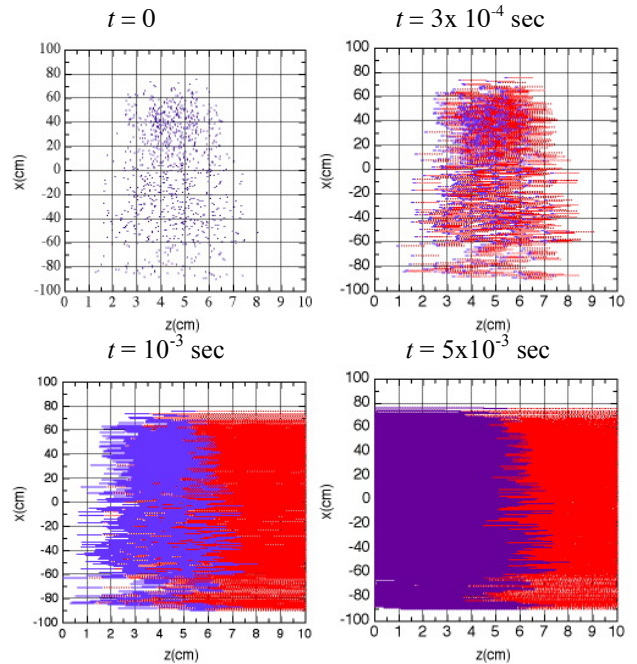


Figure 3: Time sequence of the motion of  $He^+$  ions (blue) and  $e^-$  (red) created by a  $^{79}\text{Br}$  beam at  $dN/dt_{in}=10^5 \text{ part/sec}$ . The applied (horizontal) electric field was  $10 \text{ V/cm}$ .

Table 1: Simulation Parameters

Energy per stopped ion	$1.69 \cdot 10^9 \text{ eV}$
$He^+$ mobility coefficient	$k_{He^+} = 10^5 \text{ cm}^2/\text{kVs}$
$e^-$ "mobility coefficient"	$k_e = 10^7 \text{ cm}^2/\text{kVs}$
Number of macroparticles per filling	$2 \cdot 10^3$
Number of integration steps	$5 \cdot 10^3$
Total number of macroparticles	$10^7$
Box for Poisson's equation $R \times Z$	$150 \text{ cm} \times 10 \text{ cm}$
Mesh $N_R \times N_Z$	$1024 \times 1024$

$dN/dt_{in}$ . The charged particles are considered to be extracted from the gas if they reach the walls (anode or cathode used to apply the drift field).

At significantly higher incoming beam rates, the fraction of outgoing ions becomes lower than the creation rate of ionized gas. This results from the formation of charged neutralized area in the regions of the chamber with the highest ionization densities (see Fig. 4). This limits the extraction of radioactive ions as well because some of the beam stops in the neutralized area and cannot leave the region. Fig. 4d illustrates the calculated motion of  $e^-/He^+$  ions at an incoming particle rate of  $dN/dt_{in} = 10^7 \text{ part/s}$ . This problem becomes more pronounced with increasing incoming particle rate. Figs. 5 and 6 illustrate the dependence of extraction efficiency of  $e^-/He^+$  ions as a function of the incoming charge rate for different values of buffer gas pressure and applied electric field. The space charge forces were found to significantly limit the extraction efficiency when the incoming rate exceeded  $dN/dt_{in} = 5 \cdot 10^6 \text{ part/s}$ .

The present calculations were used to estimate the total collection and extraction efficiency of radioactive beam from the cyclotron gas stopper. As a test, the actual spiral distribution of ionized buffer gas was replaced by a

uniform disk of 75 cm radius, with an axial ionization distribution centered at  $z = 5$  cm and  $\sigma_z = 1.5$  cm. Both the actual and simple distributions give a similar dependence of the extraction efficiency on the incoming particle rate. The results for the extraction of  $e/He^+$  ions were combined with the predicted stopping distribution of high energy  $^{16}O$  ions in the cyclotron stopper to obtain a total efficiency for stopping and collection. These results are shown as a function of gas pressure and incoming rate in Figs. 7 and 8. The figures show the advantage of using a cyclotron gas stopper over a traditional linear gas stopper for such high-intensity, light ion beams.

It should be noted that the present results should be considered with some caution due to the reduced electron mobility and the omission of any diffusion processes. Continued development of the cyclotron gas stopper design is underway including detailed studies of the effects of space charge on the ion motion at the RF-carpet and investigations into techniques to perform calculations with the true electron mobility.

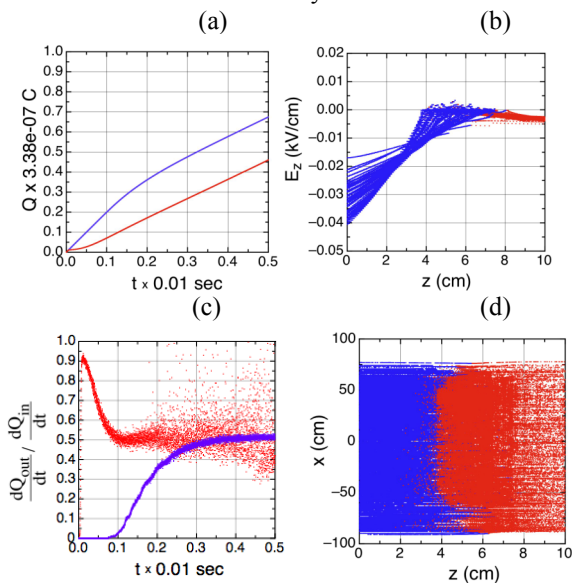


Figure 4: Conditions for space-charge neutralized plasma with  $e$ (red) and  $He^+$ (blue) at incoming beam rate of  $dN/dt_{in}=10^7$ part/s: (a) accumulated charge, (b) total electric field, (c) flux of electrons through  $z=0$  and that of  $He^+$  through  $z=10$ cm, (d) particle distribution at  $t=5 \cdot 10^{-3}$ s.

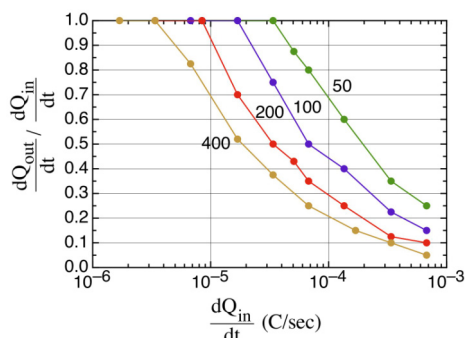


Figure 5: The fraction of extracted charge, i.e., efficiency of  $e/He^+$  extraction, as a function of incident beam rate for different values of buffer gas pressure (in mbar).

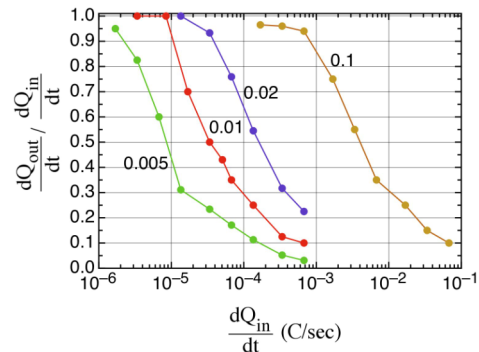


Figure 6: Similar to Fig. 5, the efficiency of  $e/He^+$  extraction as a function of Incident beam rate for different values of the applied field (in kV/cm).

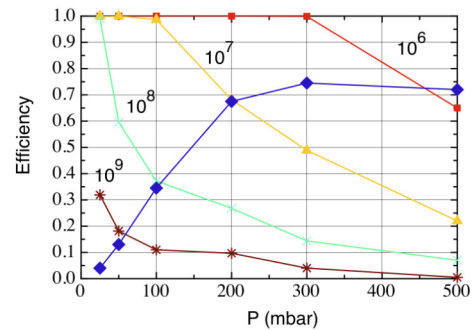


Figure 7: The collection efficiency and the total (blue diamonds) stopping efficiency for incident  $^{16}O$  heavy ions as a function of gas pressure and incoming beam rate (in part/s).

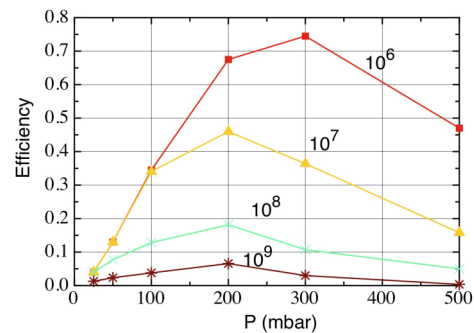


Figure 8: The total efficiency for  $^{16}O$  heavy ions as a function of gas pressure and incident beam rate (in part/s).

## REFERENCES

- [1] G. Bollen, D.J. Morrissey, S. Schwarz, Nucl. Instrum. Meth. A550, (2005) 27.
- [2] G.K.Pang, et. al, Proc. of PAC07, Albuquerque, New Mexico, USA (2007) 3588-3590.
- [3] O.Tarasov and D.Bazin, Nucl. Phys. A746 (2004) 411.
- [4] H. Weick, <http://www-linux.gsi.de/~weick/atima/>
- [5] J.F. Ziegler, <http://www.srim.org/>
- [6] C. Campbell, et al., Nucl. Instr. Meth. A, to be published.
- [7] Y.Batygin, Nucl. Instrum. Meth. A539 (2005) 455.